



ELSEVIER

Fluid Dynamics Research 24 (1999) 375–404

**FLUID DYNAMICS
RESEARCH**

Perturbed vortical layers and shear sheltering

J.C.R. Hunt^{a, *}, P.A. Durbin^b

^a*Department of Applied Mathematics & Theoretical Physics, University of Cambridge,
Silver Street, Cambridge CB3 9EW, UK*

^b*Center for Turbulence Research, Stanford University, Stanford, CA 94305-3030, USA*

Received 9 November 1998; accepted 1 February 1999

Abstract

New theoretical results and physical interpretations are presented concerning the interactions between different types of velocity fields that are separated by thin interfacial layers, where there are dynamically significant variations of vorticity across the layers and, in some cases within them. It is shown how, in different types of complex engineering and environmental flow, the strengths of these interactions vary from the weakest kind of superposition to those where they determine the flow structure, for example by mutual exclusion of velocity fields from the other region across the interface, or by local resonance near the interface. We focus here on the excluding kinds of interactions between, on the one hand, elongated and compact regions containing vortical flows and large variations in velocity, and on the other hand various kinds of weak perturbation in the surrounding external flow region: rotational, irrotational; time-varying, steady; large, small; coplanar, non-coplanar; non-diffusive, diffusive. It is shown how all these kinds of external disturbances can be wholly, or partially, ‘blocked’ at the interface with the vortical region, so that beyond a certain sheltering distance into the interior of this region the fluctuations can be very small. For the special case of quasi-parallel co-planar external straining motions outside non-directional shear flows, weak sheltering occurs if the mean velocity of the shear flow increases – otherwise the perturbations are amplified. For non-parallel flows, the sheltering effect can be greater when the vorticity is distributed in thin vortex sheets. The mechanism whereby the vortical flow induces ‘blocking’ and ‘shear-sheltering’ effects can be quantitatively explained in terms of the small adjustments of the vorticity in the vortical layers, and in some cases by the change in impulse of these layers. If the vorticity in the outer part of the vortical region is weak, it can be ‘stripped away’ by the external disturbances until the remaining vorticity is strong enough to ‘block’ the disturbances and shelter the inner flow of the vortical region. The mechanisms presented here appear to explain on the one hand some aspects of the observed robustness of vortical structures and jet or plume like shear flows in turbulent and geophysical flows, and on the other hand the levels of external perturbation needed to erode or breakdown turbulent shear flows. © 1999 Elsevier Science B.V. All rights reserved.

1. Introduction

Progressively over the past 30 years, during which the Japanese Society of Fluid Mechanics has been establishing itself very successfully, the problems studied in fluid mechanics have become

* Corresponding author.

E-mail: j.c.r.hunt@damtp.cam.ac.uk

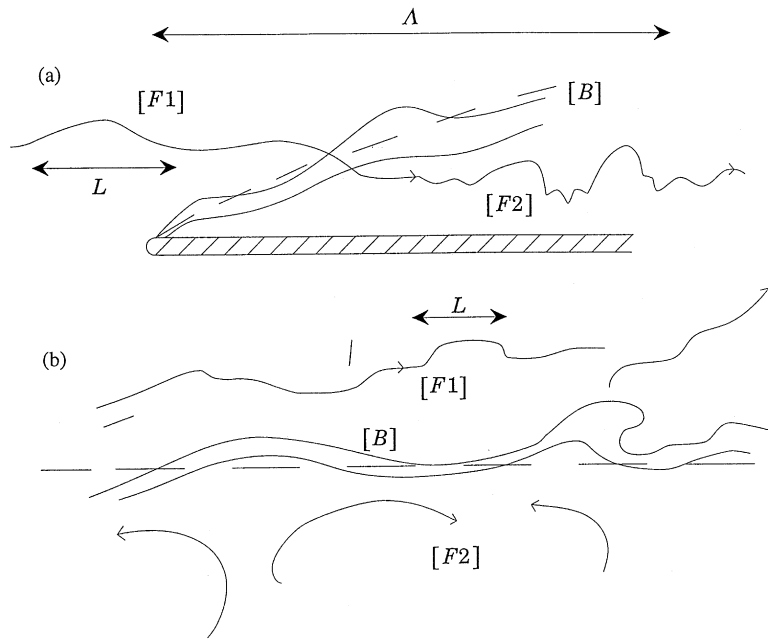


Fig. 1. Schematic diagram of interactions over a length scale Λ between an external region [F1], containing disturbances with length scale L and a vortical region [F2], that may be turbulent. The regions are separated by an interface [B] of finite thickness, whose instantaneous position is indicated by solid lines (=) and whose mean position is indicated by a dashed line (---). (a) Streamlines pass through [B], so that the interactions are advected (AI). (b) Streamlines are parallel to [B], so that the interactions are external (EI).

considerably more complex, particularly those involving different types of fluid motion in overlapping or adjacent regions of flow. We are concerned here with flows at high Reynolds and Peclet numbers, so that the effects of molecular diffusion on the interactions between these flows are small except close to the boundary [B] between them. In these more complex configurations the overall flow is not generally dominated by a single mechanism or defined by one or two dimensionless parameters, for example perturbations do not grow everywhere at the same rate (Hunt and Carruthers, 1990). However, many studies have shown that in particular zones, or thin layers, and on certain ranges of time and/or length scales the flow may be dominated by particular mechanisms which are characterised by very few parameters. In many cases these mechanisms correspond to singularities in the governing equations, which is why we should follow Tatsumi's (1999) injunction, spoken forcefully as if to a party of Samurai warriors, and 'attack the singularity'. New flow phenomena and characteristic mechanisms arise from the interactions between the flow regions, say [F1] and [F2]. These tend to develop within the flow regions when the flows cross the boundaries [B], or else in layers close to [B], whence interacting effects may propagate or be advected into the interior of the regions (Fig. 1).

A large class of such fundamental flow problems, which have many interesting practical applications are characterised by interactions between adjacent regions of turbulent velocity fields, having distinct characteristics, perhaps generated by different kinds of instability or having widely different length scales. These interactions occur within turbulent flows, and also ionised fluids, for example

where small eddies impinge on large coherent structures, or where the outer and inner parts of a turbulent boundary layer meet (e.g. Terry et al., 1992). In engineering these problems occur in the design of turbomachines. There, the flow approaching the rotating aerofoil blade or centrifugal impeller contains turbulent eddies that are much larger than the small scale turbulence in the boundary layers on the solid moving parts. In order to determine the effects of this external turbulence on heat transfer or the pressure distribution, it is necessary to understand how it affects the growth of the turbulence in the boundary layers, when they are initially laminar. Because this occurs at lower values of the Reynolds number than without external turbulence – it is called ‘bypass’ transition. Is it caused by the growth of external turbulence after being simply advected into the growing boundary layers (an advected interaction (AI)), or alternatively or simultaneously does the external turbulence directly induce pressure and velocity fluctuations in the shear profile of the boundary layer, that may be unstable? This is the problem of ‘receptivity’. The latter external interaction (EI) mechanism may be very weak because of the tendency of a shear profile to be sheltered from external fluctuations. Experiments and numerical simulations (e.g. Goldstein and Wundrow, 1998; Voke and Yang, 1995; Liu and Rodi, 1991) cannot really discriminate between these competing mechanisms without a better theoretical framework, to which we contribute in this paper. It has long been recognised that sheared interfaces strongly affect the transmission or blocking of sound. The dynamics of this process has some similarity with the dynamics of the problems considered here (Ffowcs-Williams and Purshouse, 1981).

Similar problems arise on a range of larger scales in meteorology; a major concern is whether vigorous turbulence on the scale of a kilometer driven by thermal convection in deep clouds can descend into the boundary layer flow near the ground and cause high speed gusts, or whether the vorticity of the shear flow can in any way prevent or significantly distort this process. (Collier et al., 1994; Nakamura et al., 1996).

On the even larger scale of thousands of kilometers there are well defined atmospheric motions where relatively intense regions of organised vortical motion, such as cyclonic storms or polar vortices, interact with randomly structured external disturbances. It is often found, though perhaps not very well explained yet, that the vortical regions are hardly ever penetrated by energetic large scale disturbances, and their erosion by those on smaller scales is very slow (e.g. Legras and Dritschel, 1993). This may explain why these vortical regions can persist almost undistorted for large periods (over several days or even a month) (Methven and Hoskins, 1998).

Interactions between eddy motions in adjacent regions of turbulence in geophysical flows are generally limited, by stabilising buoyancy forces and on large scales by Coriolis forces. This tends to limit the interactions to layers near [B]. But the existence of a stable layer implies that wave motions are set up which may either propagate the effects of the interaction far from [B] (Carruthers and Hunt, 1986), or may trap the wave energy that therefore steadily increases. Then the waves must break and dissipate the energy (Perera et al., 1994). A similar wave-resonant interaction (WR) tend to occur between external vortical disturbances and intense elongated vortices (Miyazaki and Hunt, 1998).

Other aspects of interactions have to be considered in flows around groups of obstacles. These might be solid immovable bluff objects, whether on a plane surface (ranging in scale from sand grains to mountains) or in cross flows, such as rows of cylinders in heat exchangers. Equally interesting group effects occur when the obstacles are free to move, as they are in disperse two-phase flows. In either type of flow the wake of each obstacle perturbs the velocity field around downstream obstacles, and also the wakes directly interact with each other (e.g. Davidson et al., 1995). Clearly there are

many interacting flow regions, so that a statistical description of the flow is generally necessary; but this still requires a good understanding of the mechanics. One effect that is implicitly assumed in current two-phase models, is that the long range effects on the flow caused by any one obstacle is much reduced by the presence of the others (Hunt et al., 1995). These sheltering effects are also significant at low Reynolds numbers (Koch, 1993).

For these types of complex flow practical models are needed; one approach is to make simplifying assumptions about the nature of the interactions (see Hunt, 1998), and classify them as broadly:

(i) superposition (S) of flows in overlapping regions so that interactions can be ignored, an example of the success of this approach, but still without much formal justification is modelling the combined forces on particles in two-phase flows (Magnaudet et al., 1995).

(ii) exclusion of flows (X), or flow processes, in certain regions because a particular mechanism is dominant, especially near the boundary [B];

(iii) significant interactions (AI and EI) between the flows in the adjoining regions, in which new phenomena or mechanisms may arise.

In this paper we focus on interactions between external flows containing perturbations and adjacent vortical flows, of and we consider how the interactions may be classified as above. We analyse in Section 2 disturbances of scale L in [F1] outside shear layers which extend over distances A in the mean flow direction, that are much greater than the scale L . We consider how the disturbances are distorted by the vorticity in [F2], and how this can lead to the flow in this region being sheltered by the shear. In Section 3 we consider cases where L is of order of A and the boundary between the regions is not planar, nor are the mean flows necessarily parallel to each other; again we note the distortion, or blocking effects, in [F1] and in some cases sheltering in [F2]. The results have interesting implications for certain global scale atmospheric motions and concepts about the inhomogeneous structure of turbulence, both on small and large scales and for statistical models.

2. Finite scale perturbations to elongated shear layers

2.1. Perturbations outside boundary layers

Our object here is to analyse the external interactions (EI) between perturbations $\mathbf{u}^{[\infty]}(\mathbf{x}, t)$ in the free-stream, where the streamwise mean velocity is $\bar{u} = U_\infty$ in the adjacent boundary layer over a rigid surface at $y=0$ and the mean velocity profile is $U(y)$. We are not considering the advected interactions (AI) of the perturbations as they enter the growing layer; in fact we assume here that the layer has constant thickness h . Thus

$$U(y) = U_\infty \tilde{U}(\tilde{y}), \quad \tilde{y} = y/h,$$

$$\tilde{U} \rightarrow 1 \quad \text{as } \tilde{y} \rightarrow \infty, \quad \tilde{U} = 0 \quad \text{at } \tilde{y} = 0. \quad (2.1)$$

We consider a relatively weak two-dimensional fluctuation with magnitude $u_0 \ll U_\infty$, with a length scale L , and it moves with a velocity c in the free stream. In order to obtain analytic solutions and demonstrate the key processes we assume that $L \gg h$; this approximation is relevant to many experiments and practical configurations. See Fig. 2. Some of the results can be generalised to three-dimensional fluctuations.

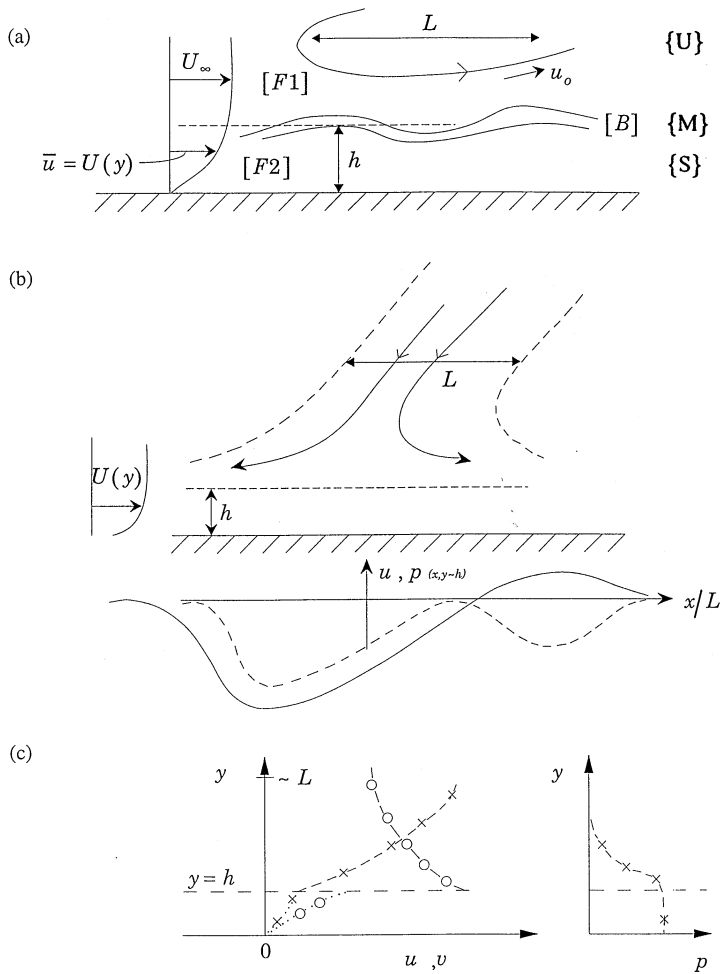


Fig. 2. External interactions between a boundary layer flow in [F2] and small amplitude disturbances travelling with the freestream speed U_∞ . (a) Schematic diagram with scales, showing the flow zones {U} in [F1] and {M}, {S} in [F2]. (b) the perturbation streamlines (—) in a moving wake travelling outside the boundary layer (after Hodson, 1988), and the profiles in the streamwise direction of the perturbation velocity u and perturbation pressure p at the top of the middle {M} zone. (c) Typical vertical profiles of the variances of the ‘blocked’ fluctuations in the horizontal (-o-o-o) and vertical (-x-x) velocity components in the zone {U}. Because of ‘shear sheltering’ the amplitudes of the velocity fluctuations in {M} are small and of second order (o.o.,x.x.x). The amplitudes of pressure (-x-x) are second order in {U} and in {M}.

Thus in the free stream, as $y/L \rightarrow \infty$, the total velocity field \mathbf{u}^* is given by $\mathbf{u}^* = \mathbf{u} + \bar{\mathbf{u}}$, where the perturbation field is expressed in moving coordinates as $\mathbf{u} = \mathbf{u}^{[\infty]} = u_0 \mathbf{f}(\hat{x}, \hat{y})$, and the mean velocity is $\bar{\mathbf{u}} = (U, 0, 0)$, where

$$\hat{x} = \frac{x - ct}{L}, \quad \hat{y} = y/L \quad \text{and} \quad \mathbf{f} = (f_x, f_y, 0) \tag{2.2}$$

either the maximum value $f_x \approx 1$ or, if it is random the rms value of $(\overline{f_x^2})^{1/2} \approx 1$, so that u_0 indicates the magnitude of the free stream disturbance. We assume that

$$u_0 \ll U_\infty. \quad (2.3)$$

We now consider how \mathbf{u} changes above and within the layer as it is advected downwind. Previous studies by Grosch and Salwen (1978) and Jacobs and Durbin (1998) have considered small disturbances, where \mathbf{f} is periodic in x and y , that travel at the same speed as the mean flow, i.e. $c = U_\infty$. They showed that, as $\text{Re}(=hU_\infty/\nu) \rightarrow \infty$, external disturbances are damped out at the top of the boundary layer. Here ν is the kinematic viscosity. If only linear disturbances are considered, they are exponentially small, below a certain sheltering distance

$$\ell_{ss} \sim h(h\text{Re}/L)^{-1/3},$$

so that as h/L decreases, ℓ_{ss}/h increases. This demonstrates the principle of shear sheltering for linear disturbances when $c = U_\infty$. What happens when these precise constraints are relaxed? The experimental evidence is that some penetration can occur.

Consider the problem of a mathematically ‘compact’ moving disturbance such that $|\mathbf{f}| \rightarrow 0$ as $|\hat{x}| \rightarrow \infty$. This could be the wake of a body moving across the stream ahead of the plate (Hodson, 1985; Liu and Rodi, 1991); in this case $f_x, f_y < 0$. Since $f_y \neq 0$ on $y = 0$, the external disturbances impact on the boundary layer and the plate. This creates an additional perturbation velocity $\Delta\mathbf{u}$, which may be analysed in three zones corresponding to different mechanisms, namely upper {U}, where $y > h$; middle {M}, where $h < y < h_s$; and surface {S} with depth h_s , where $h_s > y > 0$. As in other rapid distortion problems, the changes to the initial or free-stream disturbances are linear over a travel time $T_d = x/U_\infty$ less than the intrinsic time scale of the disturbance $T_L \sim L/u_0$. In the zone {U} above the boundary layer where vorticity comes only from the external disturbance, this vorticity field is simply advected by the mean flow and is not distorted by the changes to the perturbation velocity near the plate (Hunt and Graham, 1978). This implies that the perturbation velocity field is the sum of the initial free stream field and $\Delta\mathbf{u}$, so that

$$\mathbf{u} = \mathbf{u}^{[\infty]} + \Delta\mathbf{u}, \quad (\Delta u, \Delta v) = \nabla\phi, \quad (2.4a)$$

where, to satisfy continuity,

$$\nabla^2\phi = 0. \quad (2.4b)$$

Since the length scale of the free stream perturbation $\mathbf{u}^{[\infty]}$ is large compared to the boundary layer depth h , the boundary condition on

$$\Delta\mathbf{u} \quad \text{as} \quad y/L \rightarrow 0$$

is that

$$\Delta v_0 = \frac{\partial\phi}{\partial y}(y/L \rightarrow 0) = -u_0 f_y. \quad (2.4c)$$

In the free stream, as $y/L \rightarrow \infty$, $|\Delta\mathbf{u}| = |\nabla\phi| \rightarrow 0$. This linear calculation implies that $\Delta\mathbf{u}$ and ϕ are also functions of \hat{x} and \hat{y} and are not varying in time as they move downstream.

Note that further downstream where $T_d > T_L$ the impingement of the free stream perturbations onto the plate leads to significant distortion of their vorticity as for example occurs when vortical eddies in shear free boundary layers roll up into vortex tubes near the surface (Perot and Moin, 1995).

In the middle layer {M} the equation for the vertical velocity perturbation v is essentially the Rayleigh equation for small perturbations to a shear flow (Drazin and Reid, 1980; Collier et al., 1994). It can be expressed in coordinates moving at the speed of the disturbance c as

$$\partial^2 \hat{v} / \partial \hat{y}^2 - \hat{v} \left(\frac{d^2 U / d \hat{y}^2}{U - c} \right) = 0, \tag{2.5}$$

where $\hat{v}(\hat{x}, \hat{y}) = v(x, y, t)$, and, for consistency, $\hat{u}(\hat{x}, \hat{y}) = u(x, y, t)$. To solve Eq. (2.5) it is convenient to write $\bar{U} = U(\hat{y}) - c$, noting that $\hat{y} = \tilde{y}h/L$ and that $d^2 U / d \hat{y}^2 = d^2 \bar{U} / d \hat{y}^2 \sim U_\infty L^2 / h^2$.

If $c = U_\infty$, then $\bar{U} \rightarrow 0$ when $\hat{y} \sim h/L$ and $\bar{U} \rightarrow -c$ as $\hat{y} \rightarrow 0$.

The boundary condition on \hat{v} is that, since the vortical deflections of [B] are assumed to be small compared to h , both \hat{v} and p are continuous at the interface between {U} and {M}, i.e. where $\hat{y} \rightarrow 0$ and $\hat{y}L/h \rightarrow \infty$ (see also Section 2.3).

Following Lighthill (1957), the complete solution to Eq. (2.5) can be expressed as

$$\hat{v}(\hat{x}, \hat{y}) = -A'(\hat{x})\bar{U}(\hat{y}) - B'(\hat{x})\bar{U} \int_{\hat{y}_1}^{\hat{y}} \bar{U}^{-2}(\hat{y}^\dagger) d\hat{y}^\dagger, \tag{2.6}$$

where the prime denotes a derivative and \hat{y}^\dagger is the integration variable.

Thence, from continuity (i.e. $\partial \hat{u} / \partial \hat{x} + \partial \hat{v} / \partial \hat{y} = 0$)

$$\hat{u}(\hat{x}, \hat{y}) = A(\hat{x})\bar{U}'(\hat{y}) + B(\hat{x}) \left[\hat{U}' \int_{\hat{y}_1}^{\hat{y}} \bar{U}^{-2}(y^\dagger) dy^\dagger + \bar{U}^{-1}(\hat{y}) \right], \tag{2.7}$$

where $A(\hat{x}), B(\hat{x})$, and \hat{y}_1 are determined by satisfying the velocity and pressure conditions.

Firstly, in order that $\hat{v} = 0$ on $y = 0$, since $\bar{U}(0) \neq 0$, $A'(\hat{x}) = 0$, and $\hat{y}_1 = 0$.

In order to match with the external solution, we note that if $c = U_\infty, \bar{U} \rightarrow 0$, as $\hat{y}L/h \rightarrow \infty$. In the boundary layer, in a coordinate frame moving with speed c , the full expression for the pressure perturbation is

$$-\frac{\partial p}{\partial \hat{x}} = \bar{U} \frac{\partial \hat{u}}{\partial \hat{x}} + \hat{v} \frac{\partial \bar{U}}{\partial \hat{y}} + \left[\hat{u} \frac{\partial \hat{u}}{\partial \hat{x}} + \hat{v} \frac{\partial \hat{u}}{\partial \hat{y}} \right]. \tag{2.8}$$

Note that within {M}, provided, $\partial^2 \hat{U} / \partial \hat{y}^2 \neq 0$, the leading linear approximations can be used to calculate variations of the velocity fluctuations within the layer. These are driven by pressure fluctuations $p^{[U]}$, above the layer which may be non-linear. Here the non-linear terms are marked by the square brackets.

We now consider the case of $c = U_\infty$. Then at a small distance below the top of the layer, where $y = h_\ell$ such that $\bar{U}(h) = |U - U_\infty| > u_0$, the above equation (2.8) is dominated by the linear terms, so that the term in square brackets can be neglected. Above this level the equation is non-linear, because the linear terms are very small. Thus the results (2.6) and (2.7) are valid for $y < h_\ell$, and it follows from Eq. (2.8) that to first order

$$-\partial p / \partial \hat{x} = \partial B / \partial \hat{x}. \tag{2.9}$$

Since the distance between the levels $y = h$ and $y = h_\ell$ is much less than L , the difference in pressure is also small. To leading order $p^{[M]}$ does not vary with y in {M} and is therefore equal to its value at the bottom of the upper layer {U} above the boundary layer, whence

$$B(\hat{x}) = -p^{[M]}(\hat{x}) = -p^{[U]}(\hat{x}, \hat{y} \rightarrow 0). \tag{2.10}$$

Note that although v and p at the bottom of $\{U\}$ and at the top of the linear part of $\{M\}$ match each other, this is not the case for the horizontal component u , since the linear solution for u in $[M]$ given by Eq. (2.7) is singular as $\hat{y}h/L \rightarrow \infty$. The finite limit for \hat{v} as $\hat{y}h/L \rightarrow \infty$ for a realistic boundary layer profile, such as $U \sim U_\infty \exp(-\hat{y}L/h)$, is determined by Eq. (2.6). Thus

$$\hat{v} \sim -B'(\hat{x}) \left(\bar{U} \int_0^{\hat{y}} \bar{U}^{-2} d\hat{y}' \right), \quad \text{so that } |\hat{v}| \sim (h/L) \frac{|B(\hat{x})|}{U_\infty} \sim (h/L)(u_0^2/U_\infty). \quad (2.11)$$

Note that as $h/L \rightarrow 0$, then at the top of this thin boundary layer the vertical velocity fluctuations relative to their external level are negligible to first order. Therefore the ‘blocking’ boundary condition (2.4c) for Δv in the upper zone $\{U\}$ is effectively applicable at the level $y \sim h$. For $y < h$, the streamwise velocity fluctuation is given in terms of $p^{[M]}$ by

$$u = p^{[M]}(\hat{x}, \hat{y} \rightarrow 0) Z(\hat{y}),$$

where

$$Z = \frac{d\tilde{U}}{d\hat{y}}(\hat{y}) \int_0^{\hat{y}} \tilde{U}^{-2}(\hat{y}^\dagger) d\hat{y}^\dagger + \tilde{U}^{-1}(\hat{y}) \quad \text{and} \quad \tilde{U} = -\bar{U}/U_\infty.$$

Note that for the case where $c = U_\infty$,

$$\tilde{U} = (1 - U/U_\infty).$$

Therefore when $c = U_\infty$ at the top of $\{M\}$ non-linear or viscous processes determine the smooth transition between these layers. An approximate form for u that is finite and continuous across this narrow ‘critical’ layer at $y \sim h$, and is asymptotically correct when $L \gg y > h$ and when $y \ll h$, is

$$u(\hat{x}, \hat{y}) = \frac{-p^{[M]}(\hat{x})}{(\bar{U} - U_\infty) + \lambda(\hat{x})} \quad \text{where } \lambda = -(p^{[U]}/u)(\hat{x}, \hat{y}, \rightarrow 0) \quad \text{in } \{U\}. \quad (2.13)$$

To illustrate these effects of the blocking of the external normal velocity $v^{[\infty]}$ by the shear in the boundary layer, when $c = U_\infty$, and the sheltering of the flow within the layer, we consider a particular example of a small but finite amplitude free stream perturbation that moves with the mean velocity, and is of such a form that the pressure perturbation far above the plate is exactly zero. We take the practical example of a weak jet or wake, such that $\mathbf{u} = -(\cos \alpha, \sin \alpha)u_0 \hat{f}$ where $\hat{f} = 1/(1 + \hat{x}^2)$. This corresponds to a travelling wake impacting on the boundary layer (Hodson, 1985), if $\pi/2 > \alpha > 0$, or an atmospheric downburst if $\pi > \alpha > \pi/2$. Then for $T_d < T_L$, at the bottom of the zone $\{U\}$ just above the boundary layer the solution for ϕ in Eq. (2.4), can be written in complex form as $\Delta u - i\Delta v = \sin \alpha/(i + z)$, whence $\Delta u(\hat{x}, \hat{y} \rightarrow 0) = \lambda_u(\hat{x})u_0$, where

$$\lambda_u = (\hat{x} \sin \alpha)/(1 + \hat{x}^2). \quad (2.14)$$

In this case the streamwise velocity perturbation just above the boundary layer consists of the free stream perturbation and a forward jet on the leading side of the perturbation and a negative one on the trailing edge. See Fig. 2b.

The results (2.13) show that to first order the velocity fluctuations in zone $\{M\}$ of $[F2]$ are zero. But to second order they are finite and are determined by the pressure perturbation p at the bottom of $\{U\}$, where

$$y/L \rightarrow 0 \quad p^{[M]} = -(1/2)(u_\infty + \Delta u(y=0))^2 + \Delta p, \quad (2.15a)$$

where $\Delta p = p_{\text{stag}} + \int_{\hat{x}_{\text{stag}}}^{\hat{x}} (\partial u / \partial t) d\hat{x}$. The latter small term, which is formally of the same order as $p^{[M]}$, is the result of the distortion of the vorticity of the perturbation by the leading order ‘blocking’ term in Eq. (2.14). For a *sinusoidal* free stream perturbation this term can be calculated, in which case $p_{\text{stag}} = \frac{1}{6}u_0^2$ and the maximum value of the error Δp is $\frac{1}{3}u_0^2$.

Thus in our wake example

$$p(\hat{x}, \hat{y}/L \rightarrow 0) = p^{[M]}(\hat{x}) \simeq -\frac{1}{2}u_0^2 [(-\cos \alpha + \hat{x} \sin \alpha)/(1 + \hat{x}^2)]^2. \tag{2.15b}$$

Thence using Eq. (2.12) u can be calculated in the layer {M}. Note that its form differs from that in {U}, being everywhere negative and having two minima.

The form of the perturbation changes downstream ($T \geq T_L$), when the vorticity of the impacting disturbance begins to be significantly distorted, and higher order terms in Eq. (2.15a) have to be considered. In addition if the boundary layer is laminar, instabilities tend to be stimulated and modulated by the travelling disturbance above the layer, as recent direct numerical simulations demonstrate (Wu et al., 1999). The experimental flow studied by Liu and Rodi (1991) corresponds to that of our example, and the results for u in the early stages of the interaction are very similar to these theoretical results. Both the DNS and experiments demonstrate the sharp difference between the form and magnitude of the fluctuations in the zones {U} and {M}, showing that it is quite incorrect in these problems to seek solutions where all components grow with time throughout the flow at the same rate.

If the disturbances travel at speeds c significantly different from the free stream speed, as occurs in atmospheric downbursts, shear sheltering is limited or does not occur at all. Indeed the surface gusts may be quite large, and their form may be strikingly different from those generated in normal conditions by surface shear (Collier et al., 1994).

In terms of the concepts of interacting flows proposed in the introduction, these flows demonstrate the phenomena of exclusion (X) in some circumstances, of superposition (S) in others, depending largely on the parameter c/U_∞ , and to a lesser extent on the amplitude u_0/U_∞ . Qualitatively all the results shown here are also applicable to three-dimensional perturbations, both in terms of locking and shear sheltering. This can be shown by using the three-dimensional analysis of thin shear layers (Hunt et al., 1988) and by referring to the analysis of Craik (1991).

2.2. Shear introduced into inhomogeneous turbulence

We now consider a different type of flow where a mean shear flow is introduced (when $t > 0$) into a pre-existing field of inhomogeneous turbulence near an interface, in contrast to the previous problem where external turbulence was introduced outside an existing shear layer.

We consider how a field of low intensity turbulence in region [F1] with homogeneous vorticity $\omega^{[\infty]}(\mathbf{x}, t)$ (with a velocity scale $u_0 \ll U_\infty$), and a uniform mean velocity, U_∞ , interacts across an interface [B], at $y = 0$, with the flow in region [F2]. In this region initially at $t = 0$, there is no vorticity field and the mean velocity $\bar{u}^* = U_\infty$. Then a mean shear $d\bar{u}/dy$ is applied at $t > 0$. In this case turbulence may also have been initially generated near the interface, for example by a thin shear layer. See Fig. 3. As before we consider the high Re limit and apply appropriate matching conditions across [B]. We develop here the earlier study by Gartshore et al. (1983).

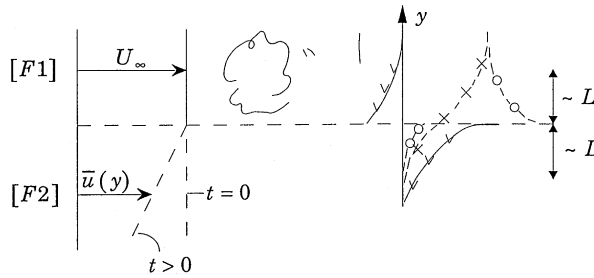


Fig. 3. Schematic diagram of the interaction between turbulence in [F1] and the flow in [F2] where a mean shear is initiated when $t > 0$, showing the difference in the profiles of $\overline{u^2}$ ($-o-o$) and $\overline{v^2}$ ($-x-x$) either side of [B] and the growth of positive and negative Reynolds stress $-\overline{uv}$ for $t > 0$ ($-v-v$).

At $t = 0$, because there is no shear in region [F2], the vorticity fluctuations in [F1] and in the locality of [B] induce velocity fluctuations at the interface at $y = 0$, namely $\mathbf{u}^{[B]}(x, y = 0, z, t)$. These in turn, induce irrotational fluctuations $\mathbf{u}^{[2]}(x, t)$ in [F2]. Since this flow must also satisfy continuity

$$\mathbf{u}^{[2]} = \nabla\phi, \quad \text{where } \nabla^2\phi = 0. \tag{2.16}$$

To satisfy the matching conditions for the normal velocity on [B], then

$$v^{[2]}(\mathbf{x}, t) = v^{[B]}(\mathbf{x}, t) \quad \text{on } y = 0. \tag{2.17}$$

Expressed in terms of Fourier components

$$v^{[B]} = A(k_1, k_3) \exp(i(k_1x + k_3z)). \tag{2.18}$$

It follows that the fluctuations in all three velocity components decrease exponentially below the interface, i.e.,

$$\text{for } y < 0, \quad |\mathbf{u}^{[2]}| \sim \exp(-k_{13}z) \quad \text{where } k_{13} = (k_1^2 + k_3^2)^{1/2}.$$

When a spectrum of velocity fluctuations at [B] is considered, whose energy increases proportionally to k^4 for eddy scales much larger than the integral scale L_X , then it is found that the energy of these fluctuations in [F2] decreases in proportion to $((-y)/L_X)^{(-4)}$. This result of Phillips (1955) was the first linear inhomogeneous RDT calculation. As with other RDT solutions which do not vary with time (or only very slowly), for long periods or distances along turbulent flows it is found to be a good approximation to the full non-linear problem and to experimental results (Hunt and Carruthers, 1990).

The statistics of the fluctuations in velocity $\mathbf{u}^{[1]}(x, z, t)$ just above the interface, even without any local generation of turbulence, differ from those of $\mathbf{u}^{[\infty]}(x, t)$ the homogeneous turbulent velocity field far above the interface, as $y/L_X \rightarrow \infty$. Firstly the difference is caused by the initial absence of vorticity fluctuations in the region [F2]; this reduces velocity fluctuations in [F1]. But secondly, since vortex lines cannot end, they are concentrated into sheets of fluctuating horizontal vorticity at the interface which increases the components of the induced velocity field parallel to the interface.

It is not clear whether the latter effect can compensate for the former reduction. To explore this question about the internal inhomogeneity within the turbulent region [F1], the RDT approximation can be used, (for $t \ll T_L$). Over this time scale the vorticity above the interface ($y > 0$) is not distorted so that the velocity field $\mathbf{u}^{[1]}$ above the interface is equal to the homogeneous field $\mathbf{u}^{[\infty]}$

plus an irrotational field $\nabla\phi^{[1]}$ caused by the distortion of the vorticity outside this domain, i.e. at the interface ($y=0$) and below it. Thus

$$\text{for } y > 0, \quad \mathbf{u}^{[1]} = \mathbf{u}^{[\infty]} + \nabla\phi^{[1]}, \quad \text{where } \nabla^2\phi^{[1]} = 0. \quad (2.19)$$

To determine $\phi^{[1]}$ and $\phi^{[2]}$ both the normal velocity and pressure fluctuation are continuous at $y=0$. This implies that the horizontal components of velocity \mathbf{u} and $\boldsymbol{\omega}$ may be discontinuous across the plane $y=0$. For small time dependent perturbations the latter condition, in conjunction with continuity, implies that the normal derivative of v is also continuous (Goldstein, 1931). This enables the amplitude function A in Eq. (2.18) to be determined in terms of the Fourier components of $\mathbf{u}^{[\infty]}$. Calculations by Carruthers and Hunt (1986) (who were mainly concerned with stratification effects) show that at $y=0$ the variance of the normal component is then about 25% of its value in the homogeneous field and that there are discontinuities in the variances of the horizontal components; above $y=0$ these components have a maximum about 12% greater than their homogeneous values; below they drop (as in Phillips' (1955) calculation) to half the value of those of the normal component). Recent conditional sampling of the velocity components at the fluctuating interface of the direct numerical simulations of a turbulent wake by Bisset et al. (1998) are consistent with this new finding, particularly the peaks in [F1] in the variances of the u and w components. In [F2] they tend slowly to the results in Eq. (2.16). Descriptive models of the large eddy structure gives a similar picture of the motions (Ferré et al., 1990). The interaction between the irrotational and vertical fluctuations either side of the interface is modelled by Townsend (1976) as inviscid flow over an elastic jelly; this may be a useful approximation for the time dependent non-linear aspects of the interaction.

When the mean shear $d\bar{u}/dy$, with mean vorticity Ω_z is introduced into region [F2] at $t=0$, it causes a growth of vorticity fluctuations. Initially the leading term in the vorticity equation is linear, so that at $t=0$,

$$d\boldsymbol{\omega}/dt = \left(\Omega \frac{\partial}{\partial z} \right) \mathbf{u}.$$

Here \mathbf{u} is initially irrotational, given by Eq. (2.16). So the usual leading term in linear calculations $(\boldsymbol{\omega} \cdot \nabla)\mathbf{u}$ is initially zero. The relative magnitudes of the velocity fluctuations induced by these growing vorticity fluctuations are similar to those in any turbulent shear flow with the eventual ordering of the magnitudes of the variances of the components being in the streamwise, transverse and normal directions respectively. Inhomogeneous, positive Reynolds shear stresses are generated in region [F2] (i.e. $(-\bar{uv}d\bar{u}/dy > 0)$), with the pressure fluctuations, as in homogeneous shear flows, making a negative contribution. Because these pressure fluctuations have a finite length scale therefore they induce a weak negative Reynolds stress in the unshered region [F1]. The former effect was measured by Gartshore et al. (1983), but the latter could not be studied because in these experiments extra wake turbulence was generated at the interface.

Comparing the results in Sections 2.1 and 2.2 shows that not only does the flow configuration affect the level and form of fluctuations across vortical layers, but it is also essential to consider the timing and sequence in which the different components of the mean and turbulent flows are introduced or generated. This can make all the difference as to whether the fluctuations are exclusive, as in shear sheltering situations, or whether mean shear co-exists with external fluctuations and then slowly interacts with it.

The concepts presented here are also relevant to explaining, the interactions in both their linear, and, by extension their non-linear aspects, between distinct and initially uncorrelated velocity fields across an interface (e.g. Fernando and Hunt, 1997), and across thin transition layers (Veeravalli and Warhaft, 1989).

2.3. Perturbations outside thin free shear layers

Consider a new flow configuration where the boundary [B] between the flow regions [F1] and [F2] is still parallel to the mean velocity $\bar{u} = U^{[1]}$. The region [F2] consists of a thin ‘free’ shear layer, of thickness such that

$$h \ll L, \quad (2.20)$$

where L is the length scale of the fluctuating velocity field $u^{[\infty]}$ introduced into [F1]. In this analysis these are considered to deflect the layer by a displacement Y that may be large compared with h , but in the linear theory is small compared with L . Across the layer there is a finite difference in mean velocity ΔU and, there is an unbounded region below it, with constant mean velocity $\bar{u} = U^{[2]} = U^{[1]} - \Delta U$. See Fig. 4.

Unlike the previous case the mean flow is now inviscidly unstable, so effectively the thickness h of zone [B] must be finite. It is determined by local turbulent shear stresses generated at the interface. However, the problem we address is to calculate the fluctuations in the region [F2] caused by external fluctuations in region [F1] that are large compared to h , using both the previous technique of matched perturbation fields, and a different approach of analysing the dynamics of these vortical boundaries; this gives more insight when there are large, unsteady non-linear distortions (e.g. Rottman et al., 1987), or when the layers are three dimensional and entraining, and possibly detraining vorticity (see Section 3.4).

If the layer is thin compared to the perturbation scale, but the amplitude of the velocity perturbation u_0 is weak enough that

$$u_0 \ll (h/L)\Delta U, \quad (2.21)$$

then any normal deflections of the layer, Y , are small compared to h . In that case the same analysis may be used as in Section 2.2, which showed how at $y=0$ on [B], for a perturbation travelling at speed c the order of magnitude of the normal velocity is given by

$$v^{[B]} \sim |U^{[1]} - c|u_0/U^{[1]} \quad \text{if } |U^{[1]} - c| \gg u_0/U^{[1]}, \quad (2.22a)$$

or

$$v^{[B]} \sim u_0^2/U^{[1]} \quad \text{if } |U^{[1]} - c| \ll u_0/U^{[1]}. \quad (2.22b)$$

Different matching conditions are needed if the condition (2.20) is satisfied, but not Eq. (2.21). The interface fluctuations $|Y|$ may be larger than h , provided they satisfy

$$L \gg |Y| > h. \quad (2.23)$$

The same perturbation analysis and matching of the interface displacement and pressure has to be used as in the well-known Kelvin–Helmholtz analysis (see Batchelor, 1967, Section 7.1).

In this case the finite displacements of the interface also deflect the mean velocity into the vertical direction, which changes the fluctuating velocity either side of the interface. In the turbulence on the

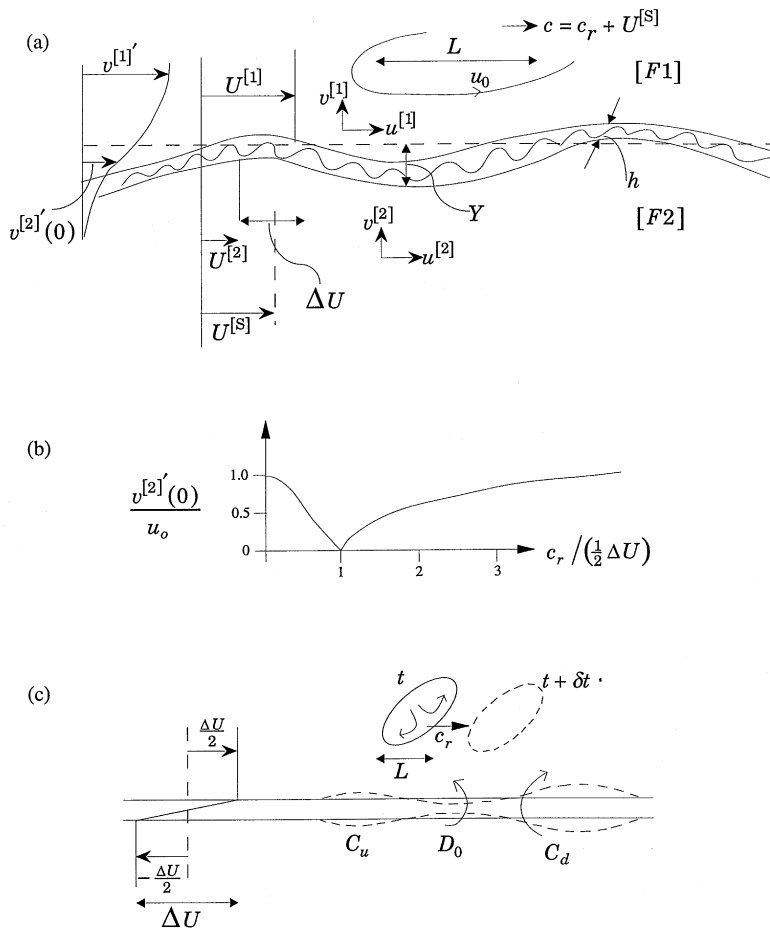


Fig. 4. (a) Free stream disturbance in [F1] travelling near a thin shear layer with a velocity c_r relative to the average velocity $U^{(S)}$ in the layer. (b) The degree of shear sheltering as defined by the rms vertical velocity fluctuation in [F2] just below the shear layer, as a function of the ratio of the relative disturbance speed c_r to the velocity jump ΔU . (c) Schematic explanation of how a vortex sheet ‘blocks’ and ‘shelters’ the velocity induced by an eddy travelling at a relative velocity c_r through strengthening the vortex sheet or convergence points C_u, C_d and reducing it at the divergence point D_0 .

‘external’ side, the RDT approximation is used, for $t \ll T_L$, to deduce that the fluctuating vorticity field is unaffected by the interface fluctuations, so that the fluctuating velocity $u^{[1]}$ is given by Eq. (2.19), as in Section 2.2. Similarly in [F2] the velocity $u^{[2]}$ is given by Eq. (2.16).

Consider the Fourier components of the two-dimensional fluctuating velocity field, having the form

$$\mathbf{u} = (\{u\}, \{v\})(k_1, y) \exp(ik_1(x - ct)), \tag{2.24a}$$

where, far above the interface, this matches the external field $\mathbf{u}^{[\infty]}$ which forces these perturbations. Thus

$$\text{as } y/L \rightarrow \infty, (\{u\}^{[1]}, \{v\}^{[1]}) \rightarrow (\{u\}^{[\infty]}, \{v\}^{[\infty]}). \tag{2.24b}$$

The same bracket notation $\{ \}$ is used for the Fourier components of other variables.

Matching the interface amplitude $\{Y\}$ and pressure $\{p\}(y=0)$ in this case leads to

$$-ik_1c\{Y\} = \{v\}^{[1]} - ik_1U^{[1]}\{Y\} = \{v\}^{[2]} - ik_1U^{[2]}\{Y\}, \tag{2.25a}$$

$$-ik_1\{p\} = ik_1(U^{[1]} - c)\{u\}^{[1]} = ik_1(U^{[2]} - c)\{u\}^{[2]}. \tag{2.25b}$$

Thence the solutions in regions [F1] and [F2] are

$$(\{\phi\}^{[1]}, \{\phi\}^{[2]}) = (B_+, B_-) \exp(-|k_1||y|) \tag{2.26}$$

where

$$k_1B_+ = (i(k_1/|k_1|)\{u\}^{[\infty]}C_-^2 + \{v\}^{[\infty]}C_+^2)/(C_+^2 + C_-^2),$$

$$k_1B_- = (i(k_1/|k_1|)\{u\}^{[\infty]} - \{v\}^{[\infty]}C_+C_-)/(C_+^2 + C_-^2),$$

where $C_+ = (1/2)\Delta U + c_r$, and $C_- = (1/2)\Delta U - c_r = U^{[1]} - c$, where c_r the relative speed of the fluctuations relative to the average velocity $U^{[S]}$ in the interface, i.e. $c_r = c - U^{[S]}$, where $U^{[S]} = (1/2)(U^{[1]} + U^{[2]})$. Note that C_- and B_- are both zero if $U_1 = c$.

Thence the rms amplitude of the normal component of the fluctuations below the interface relative to the homogeneous value is given by

$$\begin{aligned} (\overline{(v^{[2]})^2})^{1/2}/u_0 &= b \left(\frac{1}{2}\right) \left| \left(\frac{1}{4}\right) \Delta U^2 - c_r^2 \right| / \left| \left(\frac{1}{4}\right) \Delta U^2 + c_r^2 \right| \\ &\sim |U^{[1]} - c|/|U^{[1]}| \quad \text{if } |U^{[1]} - c| \ll |\Delta U|, \end{aligned} \tag{2.27}$$

where the isotropy coefficient $b = (|\{u\}^{[\infty]}|^2 + |\{v\}^{[\infty]}|^2)/(2u_0^2)$. Note how these results are consistent with Eq. (2.22) for a finite layer thickness, but small interface displacements.

The effect of shear sheltering in this case can also be explained in terms of distortion of the vortex sheet, using similar arguments as those of Batchelor (1967, Section 7.1). Let the local strength of the sheet, be defined in terms of the integral across the sheet of the z-component of total vorticity ω_3^* , as $\gamma^*(s, t) = \int \omega_3^* dn$. The strength $\gamma^*(s, t)$ varies along the flow direction s and tends to increase with time where the total streamwise velocity (averaged across the sheet) decreases, i.e. $du^{[S]*}/ds < 0$, so that the flow in the sheet converges and it thickens; γ^* decreases where $du^{[S]*}/ds > 0$. Kelvin’s theorem shows that the circulation around a line element ($\gamma^*d\ell$) is not changed in this two-dimensional flow, so the equation for γ^* is

$$(\partial/\partial t + u^{[S]*}\partial/\partial s)\gamma^* = -\gamma^*\partial u^{[S]*}/\partial s. \tag{2.28a}$$

For small deflections, there are mean and fluctuating components of the streamwise velocity averaged across the vortex sheet, and of the strength denoted, respectively, by

$$u^{[S]*} = U^{[S]} + u^{[S]}, \quad \text{where } u^{[S]} = (u^{[1]} + u^{[2]})/2 \tag{2.28b}$$

and

$$\gamma^* = \Gamma + \gamma, \quad \text{where } \Gamma = -\Delta U. \tag{2.28c}$$

Thence (2.28) becomes to leading order,

$$(\partial/\partial t + U^{[S]}\partial/\partial x)\gamma = -\Gamma\partial u^{[S]}/\partial x. \tag{2.28d}$$

In the Kelvin–Helmholtz problem these fluctuations arise from the growing eigen solution, and not from any imposed disturbance.

In our problem we consider the distortion to γ^* starting at time t , where in Eq. (2.8d) $u^{(S)}$ is the velocity induced by a vortical eddy with velocity u_0 and length L moving along a sheet with speed c . It is convenient to use a coordinate frame moving with the mean velocity in the shear layer $U^{[S]}$, so that $|\Gamma| = 2U^{[1]}$. See Fig. 4(c).

The velocity field of the eddy induces points of convergence C_u and C_d a distance of order L upstream and downstream of the eddy, and of divergence D_0 on the centreline. At these points at time t , γ^* begins to increase/decrease at a rate given by (2.28d) of order $U^{[1]}u_0/L$. By a time $t + \Delta t$ later, when the vortex has moved by a distance $\delta X = c \delta t$, the vortex sheet at C_d and D_0 has thickened, and thinned, so that the perturbation to the sheet strength γ_d is of order $\delta t U^{[1]}u_0/L$. Then an upward perturbation velocity, δv_y , is induced by this localised vortex with circulation γ_d . This can ‘block’ the downward velocity induced by the eddy at the interface, provided firstly that the induced velocity, δv_y , is comparable to u_0 , i.e. if $\delta t U^{[1]}u_0/L \sim u_0$, and secondly that this induced velocity is induced at the right place and scale in relation to the velocity of the eddy, i.e. if $\delta X \sim L$. These two conditions for blocking in [F1] and shear sheltering in [F2] are satisfied if $\delta t U^{[1]}u_0/\delta X \sim u_0$ or $\delta t U^{[1]}/c \delta t \sim 1$, whence $c \sim U^{[1]}$.

It is also clear that if the eddy moved very slowly relative to the flow i.e. $c \ll U^{[1]}$, the velocity induced by the distortion of the sheet at C_u , C_d and D_0 would not block the velocity induced by the vortex at $y=0$, and the flow in [F2] would not be sheltered.

The overall effects on the flow of these interactions can be further explored by calculating the changes to the integrals of the momentum, or ‘partial impulses’, of the fluid above and below the plane of the vortex sheet. Consider a two- or three-dimensional vortical eddy with characteristic length scale L and internal velocity u_0 , moving at a horizontal speed c and vertical velocity $v^{[\infty]} \sim u_0$, near a strong vortex sheet, such that

$$u_0 \ll |\Gamma| = \Delta U \quad \text{at } y = 0. \tag{2.29}$$

We have seen that the vortex sheet can block the vertical momentum of nearby vortical eddies. In that case, since it is not a rigid surface, the perturbed vortex sheet should have an upward momentum or impulse $I_2^{[S]}$ related to that of the eddy (but not equal, as the analysis shows). This can be proved by calculating $I^{[S]}$ in terms of the vorticity $\omega^{[S]}$ within the volume $\mathcal{V}^{[S]}$ occupied by the sheet, viz:

$$I^{[S]} = (1/(N - 1)) \int (\hat{x} \wedge \omega^{[S]}(\hat{x}) d\hat{x}, \tag{2.30a}$$

where N is the number of dimensions of the flow (either 2 or 3) (see Saffman, 1992; Batchelor, 1967). Since the sheet is very thin $\omega^{[S]}$ can be expressed as the product of a delta function and the strength γ^* of the sheet, which, in three dimensions, is a vector.

We focus on the case where the sheet ‘blocks’ the eddy, so that it has a small vertical deflection. Thence

$$\omega^{[S]} = \gamma(x, y, t) \delta(y - y'). \tag{2.30b}$$

For a three-dimensional eddy, Eq. (2.28d) for the perturbations to the strength of the sheet has two components. Writing them in a frame of reference moving at the mean velocity in the sheet, $U^{[S]}$, they are

$$\partial/\partial t(\gamma_x, \gamma_z) = \Gamma_3(\partial u^{[S]}/\partial z, -\partial u^{[S]}/\partial x), \tag{2.31}$$

where the mean strength is $\Gamma_3 = -\Delta U$. When the sheet ‘blocks’ the turbulence and shelters region [F2], the velocity fluctuations in the sheet are determined by the velocity in [F1], i.e.

$u^{[S]} = (1/2)u^{[1]}(y=0)$. But if the sheet is exactly ‘blocking’ the imposed velocity field $\mathbf{u}^{[\infty]}$, the sheet effectively adds the symmetric field of an image eddy below the interface. Therefore $u^{[1]}(y=0) = 2u^{[\infty]}(y=0)$. Because the solution to Eq. (2.31) is ‘forced’ by the perturbation velocity $\mathbf{u}^{[\infty]}(x, t, z)$, it also is translated with the eddy speed c , so that $\partial\gamma/\partial t = -c_r\partial\gamma/\partial x$. It can now be expressed in terms of the undisturbed eddy velocity field $u^{[\infty]}$ on $(y=0)$. Note that outside the vortical region of the eddy (see Fig. 4(c)) is an irrotational field, because the eddy is assumed to be above the interface. Thus near $y=0$, the perturbation velocity, is $u^{[\infty]}$, $w^{[\infty]} = \partial\phi^{[\infty]}/\partial x$, $\partial\phi^{[\infty]}/\partial z$. Thence $\partial u^{[S]}/\partial z = \partial w^{[\infty]}/\partial x$, and $\partial u^{[S]}/\partial x = \partial u^{[\infty]}/\partial x$. Collecting these results leads to the perturbations in the vortex sheet of

$$(\gamma_x, \gamma_z) = (\Delta U/c_r)(w^{[\infty]}, -u^{[\infty]})(x - ct, y=0, z). \quad (2.32)$$

Thence the vertical impulse produced by the sheet for a two and three-dimensional eddy, respectively, are

$$I_2^{[S]} = (\Delta U/c_r) \left(\int_{-\infty}^{\infty} \phi^{[\infty]}(x, y=0) dx, \int_{-\infty}^{\infty} \int_{-\infty}^{\infty} \phi^{[\infty]}(x, y=0, z) dx dz \right), \quad (2.33)$$

noting that the contribution in the three-dimensional case from the perturbed vorticity in the stream-wise direction is equal to that produced by that in the spanwise direction. Hence the coefficient is the same for both cases.

By now calculating the change in the impulse when the vortex sheet is introduced, leads to the appropriate value of c to be consistent with the assumption of an undisturbed sheet, that blocks the eddy. Initially, a two-dimensional ‘compact’ eddy, which is moving vertically with velocity $v^{[\infty]}$, has a vertical component of impulse $I_2^{[\infty]}$. For the eddy to be blocked, the sheet must exert an impulse $I_2^{[S]}$. This must be equal to the sum of the deficit of the eddy’s impulse in region [F2] and the impulse of the velocity field above $y=0$ of the image eddy located below $y=0$. For an eddy far above the interface, which is assumed in this linear analysis, it follows that

$$I_2^{[S]} = -2I_2^{[\infty]}. \quad (2.34)$$

We note that for a two dimensional eddy, or vortical disturbance, located above $y=0$, its impulse can be expressed in terms of its potential on $y=0$, so that $I_2^{[\infty]} = \int \phi^{[\infty]}(x, y=0) dx$. Therefore Eq. (2.34) is satisfied and the vortex sheet can block the eddy if $\Delta U/c_r = 2$ or $c = U^{[1]}$, which is consistent with Eqs. (2.22) and (2.27). For a three-dimensional eddy far above the sheet and moving towards it, whose velocity field is similar to that of a sphere, the reverse impulse provided by the sheet has to be $3I_2^{[\infty]}$ (for an explanation of how ‘blocking’ changes the upward and downward displacements of material surfaces see Eames et al. (1996). This condition is consistent with Eq. (2.33) if, also, $c = U^{[1]}$. We note that if the eddy is close to the sheet the impulse calculation is incorrect, and the effectiveness of blocking and shear sheltering is reduced, even if the eddy moves with the stream speed.

The blocking effect of a vortex sheet on irrotational fluctuations is a well known phenomenon in aero-acoustics (e.g. Ffowcs-Williams and Purshouse 1981), but has not been applied more generally in fluid flows, nor to turbulent flows. A remarkable geophysical example of these effects has been studied numerically by Zehnder et al. (1998). They have shown how the damaging vortex motions of tropical cyclones, when they are generated off the mountains of southern Mexico, are ‘blocked’ and strengthen as they move towards the intense shear layer of the inter-tropical convergence zone.

The blocking of external eddies by the shear layer, may amplify the interaction with the naturally growing disturbances in the shear layer. As the shear layer thickness h grows, it means that the blocking/sheltering mechanism is only relevant for external eddies, that are larger than h . This is consistent with the observations that when large scale turbulent eddies impinge onto bluff bodies and interact with the free shear layer of the wake, on the one hand, they can amplify the vortex shedding, but on the other hand they do not induce significant fluctuations within the wake (e.g. Britter et al., 1979).

These mechanisms may also explain some laboratory measurements, as well as field observations that in atmospheric turbulent boundary layers, below the level of the roughness elements (e.g. trees, or buildings), where there is a strong free shear layer, the turbulence is effectively sheltered from the low frequency and large scale fluctuations above this level. There is a corresponding blocking effect of large eddies above the lower sheltered layer which is consistent with the observation that the boundary layer above the roughness elements is displaced by a height, d , about equal to the height of the free shear layer (e.g. Jackson, 1981; Rotach, 1993).

3. Large scale distortions of finite sized vortical regions

3.1. Defining the problems

We consider here ‘compact’ vortical regions, [F2] in our notation, with characteristic vorticity Ω_0 confined within a finite length h , and immersed within an external region, [F1], in which there are large scale straining motions $\mathbf{u}^{[1]}$ superimposed on a mean flow with the same average velocity U_∞ (to first order) as that of the vortical regions. The spatial variations over distances of order L of the external velocity fields, $\mathbf{u}^{[1]}(x, t)$ are typically of order ΔU_∞ . In general, L is at least as large as h . Because of their large scales the external motions change slowly compared with the time scale $T_L^{[2]}$ of the vortical flows in [F2]. If they are not in an overall state of equilibrium (which may be statistical if the flow is turbulent) $T_L^{[2]}$ is usually determined by the internal instabilities and by the non-linear evolution of the vorticity in [F2] and is of the order Ω_0 (e.g. Versicco et al., 1995; Kevlahan and Hunt, 1997). The typical strain rate of the external flows is $\Delta U_\infty/L$. Because of the slow time variations in [F1] there are significant variations in pressure $p^{[1]}$ which are of order $\Delta U_\infty U_\infty$. By contrast in Section 2 external disturbances were advected by the background flow leading to $p^{[1]}$ being zero, to first order, and to the occurrence of shear sheltering in [F2].

These large scale straining motions also influence the overall structure of the vortical flows in [F2] by vorticity deformation mechanisms, which differ in some respects from those considered in Section 2. In particular, the interactions can now be analysed in the steady state, and consideration of the external pressure variations may not provide much guidance.

Except in Section 3.4, we focus on relatively weak inviscid external (EI) interactions (for $t > t_0$) either side of the mean boundary [B] across which no vorticity is transported.

In the analysis of Section 3.2 we first consider how two-dimensional (or axisymmetric non-rotating) vortical flows in [F2] interact with external flows that are coplanar. In order to calculate these interactions explicitly and to understand how they apply to the typically complex internal structure of vortical eddies (such as are found on all scales of high Reynolds number, turbulent and non-turbulent flow), we assume that the vorticity in [F2] is distributed in thin layers (see Pullin and

Saffman, 1998; Kevlahan and Farge, 1997). In two-dimensional interactions the vorticity component ω_z in the z -direction cannot be amplified or reorientated, but its distribution is changed, as in the two-dimensional examples considered in Sections 2.1 and 2.3.

When the straining motions of the external and vortical flows are not coplanar, the direction and amplitude of vorticity in [F2] is changed, and the interactions are more complex. Even so, it appears in Section 3.3 that the flow in [F2] may still be sheltered from the effects of the external strain where the vorticity is distributed in these layers, but not if it is continuously distributed.

The effects of finite amplitude interactions, inhomogeneity of vorticity in [F2] and large distortions of the interface are considered in Section 3.4, together with some mention of how the small scale viscous diffusions of vorticity may also affect transport on a larger scale.

3.2. Coplanar external flows and vorticity redistribution

Consider a steady unidirectional external steady flow in region [F1], defined as $y < 0$, with velocity field $(u^{[1]}, v^{[1]})(x, y)$, that is parallel to the interface [B] $y = 0$, so that $v^{[1]}(x, y = 0) = 0$. The external streamwise velocity changes along this line by a factor A_0^\dagger , so that $u^{[1]}(x, y = 0) = U(x)$, where $U(x = 0) = U_0$, and $A_0^\dagger = U/U_0$. Let $A_0^\dagger = 1 + a_0^\dagger$, where $a_0^\dagger(x)$ varies on a scale L . Because of changes to the flow [F2], the velocity field in [F1] is also slightly perturbed by $O(\epsilon a_0^\dagger)$, where the small parameter ϵ is determined after the leading order terms have been calculated.

In [F2], the initial profile of the streamwise velocity on the line $x = 0$, $u^{[2]}(y)$, is a parallel set of vortex sheets of strength $G_n (= g_n U_0)$ separated by layers of depth h_n ($n \leq N$), located at

$$y_{(n-1)} = y_N - \sum_n^N h_k \quad \text{where } y_N = 0 \text{ and } y_n < 0, \tag{3.1}$$

so that

$$u^{[2]}(x = 0, y) = U_0 \left(1 - \left\{ \sum_n^N (g_k(x = 0) H(y - y_{(k-1)})) \right\} \right). \tag{3.2}$$

Here, following the usual definition for the step function, $H(y) = 1, 0$ for $y > 0, y < 0$, respectively. As the external flow accelerates/decelerates, these vortex sheets vary in strength so that $g_n(x) = A_n(x) g_n(x = 0)$. The depths of the layers between the sheets also vary. Let the characteristic value of g_n be g_c (which may be positive or negative). For a simple demonstration of the sheltering effect, we assume that the vortex sheets are weak and that the change in the external flow is small, so that

$$a_0^\dagger \ll 1 \quad \text{and} \quad \left| \sum_1^N g_n \right| = N g_0 \ll 1, \quad \text{where we assume } |a_0^\dagger| \gg g_0 \text{ and } |g_n - g_{n-1}| \ll |g_n|. \tag{3.3}$$

As in Eq. (2.28a) we consider how line elements $dl(x)$ are extended by the total velocity $u^{*[S]}(x)$ on each sheet, so that

$$g_n(x)/g_n(0) = dl(0)/dl(x) = u^{*[S]}(0)/u^{*[S]}(x), \tag{3.4}$$

change in the pressure in [F1], namely

$$p^{[1]}(x, y = 0) - p^{[1]}(0, 0) = -a_0^\dagger U_0^2 \quad (3.8)$$

so that from Eqs. (2.7) and (2.9), for a slow varying profile in [F2],

$$u^{[2]}(x, y) - u^{[2]}(0) = a(y)u^{[2]}(0, y) \simeq a_0^\dagger U_0^2 / u^{[2]}(0, y). \quad (3.9)$$

Thus if the initial velocity profile in [F2], $u^{[2]}(0, y)$, decreases from [B] as $|y|$ increases (as in a boundary layer) then $a(y)$ increases, as $|y|$ increases. On the other hand, if $u^{[2]}(x = 0, y)$ rapidly increases, as with a jet, the effect of the external large scale perturbation decreases in proportion to $U_0/U^{[2]}$.

This conclusion is quite consistent with the observation that wakes are very sensitive to low amplitude large scale external straining and turbulences (Risso, private communication, 1995) but jets and plumes are much less so (Ching et al., 1995).

We now consider two other characteristic features of ‘compact’ vortical regions [F2]. Firstly they have curved boundaries, along which the external straining motions vary in strength and even direction. Secondly they usually go through a phase in their ‘life cycle’ when their boundaries are open, for example when vortices in shear layers grow by ‘rolling up’. In this phase streamlines enter into the interior of [F2], entraining fluid with small vorticity, and other fluid properties of the external region [F1]. As a result the vorticity distribution in [F2] tends to be highly non-uniform, and also the interface [B] has to be specially defined; for example as a contour where the vorticity has a magnitude characteristic of the region as a whole (see Townsend, 1976).

In order to study the interactions between external straining and a vortical region with such a typically complex structure, it is useful to idealise its structure as a set of concentric rings of radius R , having a high level of vorticity whose integral (or sheet strength) is γ_0^* . These surround an inner vortex core (Kevlahan and Farge, 1997). The external strain is a weak stagnation flow with velocity U_0 varying over a large length scale L ($> R$); thus its strain rate is $S \sim U_0/L$, where $SR \ll \gamma_0^*$. See Fig. 6(b).

The same order of magnitude analysis of Batchelor, as used in Section 2.3, for the response of a vortex sheet to coplanar straining motions, can be applied to this problem. When the strain is applied, the surface velocity $u^{*[S]}$ diverges (i.e. $du^{*[S]}/ds > 0$) at A^+, A^- , and therefore the local sheet strength γ^* decreases, at a rate $S\gamma_0^*$. Correspondingly it increases at the same rate at B^+, B^- . But, in this flow unlike that in Section 2.3, these perturbations in the vortex strength are advected by the mean velocity in the concentric vortex over a time Δt by a distance of order $(1/2)\gamma_0^*\Delta t$ to points denoted by $A^{+'}, A^{-'}, B^{+'}, B^{-'}$. The vertical and horizontal velocity components induced on the axes of the ring at A^+ etc., by the displaced vorticity perturbations, are of order $S\gamma_0^*\Delta t$. These are approximately equal to those of the imposed external velocity ($\sim SR$), provided that firstly the points $A^{+'}$, etc. are located near the 45° symmetry points, i.e. $(1/2)\gamma_0^*\Delta t \sim R$, and secondly that the induced velocity is large enough that $S\gamma_0^*\Delta t \sim SR$. Clearly both conditions are satisfied if $\Delta t \sim R/\gamma_0^*$. This shows why, as the outer vortex rotates, it is being strained and distorted at just the correct rate to shelter the inner vortex ring, or the inner ‘arms’ of a spiral, as the numerical computations of Kevlahan and Farge (1997) nicely demonstrate.

This assumes that there is sufficient separation between the outer and inner vortex rings, because otherwise the velocity induced by the distortion of the outer vortex will distort the inner vortices, and the sheltering would be reduced.

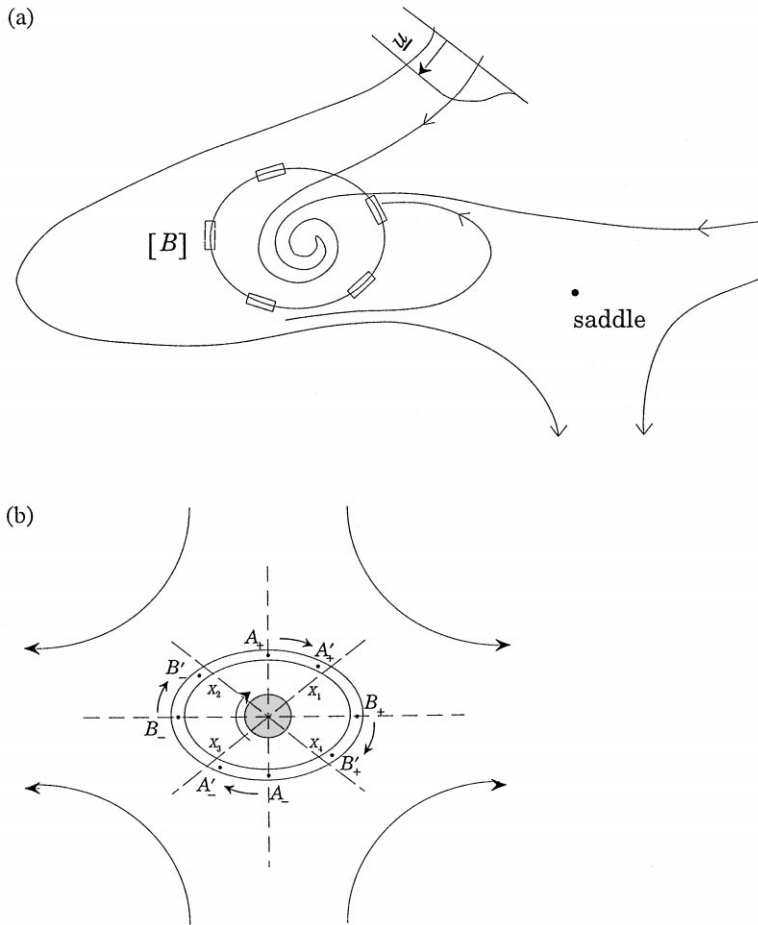


Fig. 6. Interaction between [F1] and [F2] when the boundary interface is curved. (a) Rolling up shear layers and [B] is an open surface; (b) approximation to (a) with the shear layers idealised as vortex rings (following Kevlahan and Farge, 1997).

3.3. Three-dimensional vortical interactions with swirl

Within most compact vortical regions in three-dimensional flows, the vorticity field ω is twisted and non-uniform. For example in an elongated laminar or turbulent vortex, with a flow parallel to its axis, and varying slowly along it, the vorticity has three components $\omega = (\omega_r, \omega_\theta, \omega_z)$, which in the most rapidly developing stage of the vortex is localised on vortex sheets that are rolling up concentrically. Here the radial component ω_r is proportional to the weak radial velocity and a slow change in cross sectional area (e.g. Lundgren, 1982). For this case, and for three-dimensional vortices in general, the vorticity in [F2] also induces an external irrotational flow field in [F1], over a distance of the order of the length scale of [F2], namely h . These self-induced straining motions span the regions [F1] and [F2], but only ‘react’ back on the vorticity when it is in a developing stage, and not when it is close to a steady state.

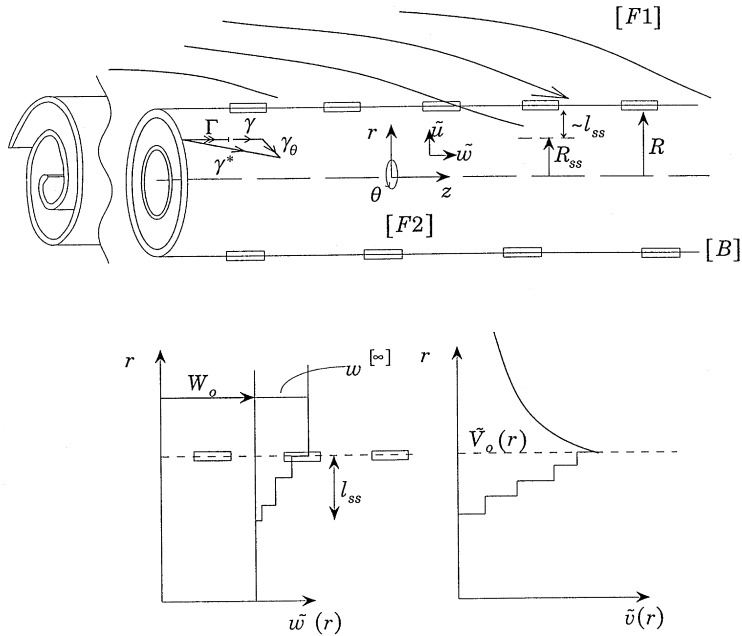


Fig. 7. (a) Schematic diagram of vortex sheets with external strains, idealised as in Fig. 6. Note how the external flow only penetrates a distance l_{ss} , as a result of the vorticity being strained in axial and azimuthal directions. (b) Typical axial and azimuthal velocity perturbations showing shear sheltering below a depth l_{ss} .

So the key question in complex flows concerns how any additional or imposed external strains in [F1] distort the vorticity in [F2]. We examine here the new aspects of these interactions when the external and vortical flows are not co-planar, the boundaries are curved and the vorticity in [F2] is non-uniform. We consider, as an example, the perturbations $\mathbf{u}(\mathbf{x})$ in both regions caused by introducing into the external region [F1], where there is a uniform stream with velocity W_0 , a weak steady axisymmetric converging flow, with characteristic velocity ΔW_0 over a length L (see Fig. 7). (This might be induced by a pair of vortex rings some distance from the interface [B].) The initial flow in [F2], $U(x)$, is induced by N concentric vortex sheets, with strength $\Gamma^{(n)}$ ($N > n > 1$). The radius of this vortical region is R ; L is the length scale of the velocity field in [F1].

Thus the total velocity is given by

$$\mathbf{u}^*(x) = \mathbf{U}(x) + \mathbf{u}(x). \tag{3.8a}$$

In cylindrical coordinates (r, θ, z) , the velocity components are denoted by tildes, i.e. $(\tilde{u}, \tilde{v}, \tilde{w})$. Thus in [F1], for $r > R$, $\mathbf{U}(x) = (0, (R/r)\tilde{V}_0, W_0)$

$$\text{for } R > r > r_1, \quad \mathbf{U}(x) = (0, \tilde{V}^{[2]}(r), W_0) \tag{3.8b}$$

where

$$\tilde{V}_0 = \tilde{V}^{[2]}(r=R), \quad \tilde{V}^{[2]}(r) = \sum_1^N \Gamma^{(k)}(r_k/r)H(r - r_k). \tag{3.8c}$$

The spacing between the sheets is h_k , which are located at $r_n = R - \sum_{n+1}^N h_k$, for $n < N$.

As an illustrative example, the external straining motion is taken to have the form

$$\mathbf{u}^{[\infty]}(x) = (\tilde{u}^{[\infty]}, 0, \tilde{w}^{[\infty]})(r, z), \tag{3.9a}$$

where

$$\tilde{w}^{[\infty]} = (z/L)\Delta W_0, \tag{3.9b}$$

and by continuity,

$$\tilde{u}^{[\infty]}(r) = - (1/r) \int_{R_{ss}}^r (\Delta W_0/L)(r^\dagger) dr^\dagger. \tag{3.9c}$$

Note that at this stage we do not know the lower limit of integration $R_{ss} (= R - \ell_{ss})$, which is the effective ‘blocking’ radius of the vortex within which the perturbation flow is sheltered by the shear from the external strain. Thence from Eq. (3.9c) the radial velocity at the outer boundary of the vortex $\tilde{u} (r = R)$ is of order $-\ell_{ss}\Delta W_0/L$.

For this axisymmetric flow the two components of the perturbation, $\gamma^{(N)}$, of the strength of the outer vortex sheet are given (to leading order) by

$$W_0 \frac{\partial \gamma^{[N]}}{\partial z} = \Gamma^{(N)} \left[\frac{\partial \tilde{w}^{[s]}}{\partial z} + \frac{\partial \tilde{u}^{[s]}}{\partial r} \right] = - \Gamma^{(N)} \left(\frac{\tilde{u}}{r} \right) \quad (r = R), \tag{3.10a}$$

$$W_0 \frac{\partial \gamma_\theta^{[N]}}{\partial z} = \Gamma^{(N)} \left[\frac{\partial \tilde{v}^{[r]}}{\partial z} \right] \quad (r = R). \tag{3.10b}$$

Note that Eq. (3.10a) is consistent with the constancy of the flux of axial vorticity in the vortex sheet $2\pi r \tilde{v}(r, z)$, and with Eq. (2.31), which showed that any straining motion parallel to the vorticity of a plane-sheet (where $R \rightarrow \infty$) does not change its strength.

It follows from Eq. (3.10a) that the negative radial velocity component \tilde{u} at the outer radius R causes the swirl velocity component just inside the vortex sheet to increase by

$$\tilde{v} \sim - \left(\frac{z}{W_0} \right) \Gamma^{(N)} \left(\frac{\ell_{ss}}{L} \right) \Delta W_0/R. \tag{3.11}$$

From Eq. (3.10b) it follows also that an azimuthal component of vorticity is generated, which leads to a reduction of the axial velocity perturbation from its value $w^{[1]} (r = R)$ in the external flow [F1] just outside the vortex, so that in [F2]

$$(\tilde{w}^{[1]} - \tilde{w}^{[2]})(r = R) = \gamma_\theta^{(N)} \sim \frac{z\Gamma^{(N)}}{W_0} \left(\frac{\partial \tilde{v}}{\partial z} \right) \sim \frac{\Gamma^{(N)^2} \ell_{ss} \Delta W_0}{W_0^2 LR} Z. \tag{3.12a}$$

Because of this reduction in \tilde{w}^* and therefore $d\tilde{w}^*/dz$ within the first layer of the vortex spiral, at the position of the next sheet, firstly the radial velocity $\tilde{u} (r = R - h/N)$ is reduced correspondingly, following Eq. (3.9c), and secondly, from Eq. (3.10a), the stretching of Γ_z is reduced. This sequence continues for a finite number N_{ss} of sheets at decreasing radial positions, until at $r = R - \ell_{ss}$, where

$N_{ss} \sim \ell_{ss}/h$, the reduction in \tilde{w} is equal to the perturbation produced by the external flow, i.e.

$$\sum_{N-N_{ss}}^N \gamma_{\theta}^{(n)} \sim w^{[1]}(r=R) \sim z\Delta W_0/L. \quad (3.12b)$$

Thence from Eq. (3.12a) the shear-sheltering depth is given approximately by

$$\ell_{ss}/R \sim (h/R)^{1/2}/(\Gamma/W_0) \sim \sqrt{R/h} \left(\frac{W_0}{\tilde{V}_0} \right), \quad (3.13)$$

where the maximum swirl velocity $\tilde{V}_0 \sim N\Gamma \sim (R/h)\Gamma$ where Γ is a characteristic value of $\Gamma^{(k)}$. This depth is, as in the previous analysis, independent of the external strain, when it is small. Note how the mechanism also can operate when the external disturbance velocity field is not coplanar, provided the interface is curved. However as the thickness of the layers between the sheets decreases the sheltering depth increases (for given ratio of the swirl to axial velocities). This is consistent with the well known result that sheltering does not operate when the vorticity is continuous, because then waves are generated within [F2] which propagate into the interior from the interface (Batchelor, 1967; Marshall, 1997). This is analogous to the change from the trapping to the propagation of internal waves in stratified flow when multiple inversion layers are close enough that they approximate to a continuous stratification, and the ‘evanescent’ decrease between the layers is negligible.

Previous studies of rolled up vortex sheets in straining flows have been focussed on their early development, when the external perturbation velocity W_0 over the length L of the vortex is comparable with the strength of the vortex sheet Γ (Lundgren, 1982), so that the external straining is unaffected by the presence of the vortex sheets. The discussion here suggests that this may not be an appropriate assumption for the next stage when the vorticity has been amplified to the extent that the swirl velocity V_0 exceeds the axial velocity W_0 . This would be consistent with the remarkable robustness, in the presence of arbitrary large scale straining motions, of the structure of small scale turbulence, which is normally attributed simply to its higher intensity rather than to any structural property (cf. Hunt and Vassilicos, 1993; Terry et al., 1992). Of course, in the final stages of existence of such vortices, when the vorticity has diffused throughout the vortical region, then again the external strain acts throughout this region and there is no sheltering (e.g. Moffat et al., 1995).

3.4. Large displacements and diffusion of vorticity

In our previous analysis it was assumed that across the bounding interface [B] between the external region [F1] and the vortical region [F2], the vorticity $\omega^{[2]}$ in the latter decreases abruptly to a much lower level in [F1]. However, in many vortical regions there is a gradual decrease in the magnitude of $\omega^{[2]}$ from its characteristic value ω_c in the core to a significantly lower value ω_B near the interface [B], which is comparable with or smaller than the strain rate in the external region [F1]. Using the results of Dritschel and Legras (1993) we analyse here the mechanisms for how in these flows external perturbations in [F1] cause large distortions and displacements of the interface [B] over distances of order h , the length scale of [F2]. They also cause changes to the vorticity field in [F2] that are large in the outer part, and small though significant in the core. Such interactions, involving a different type of inhomogeneity in [F2], play a critical role in the formation and persistence of

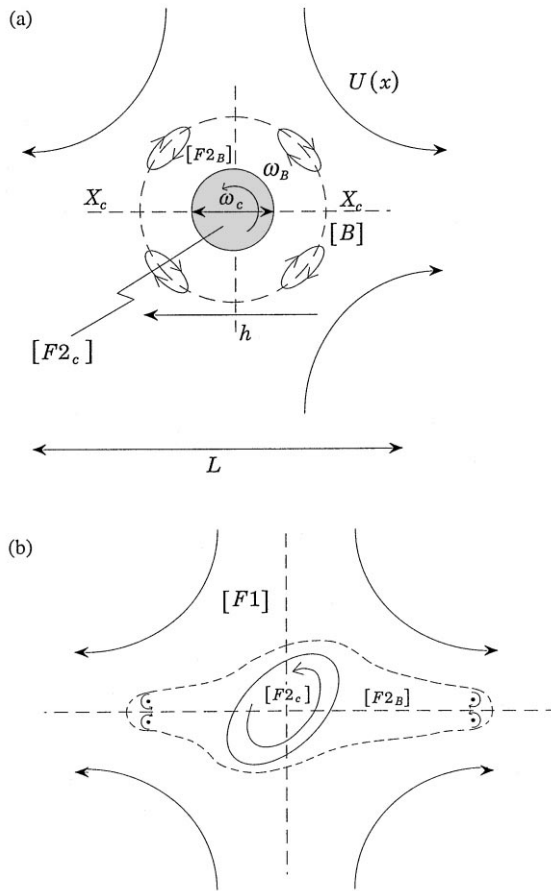


Fig. 8. Schematic diagram of the mechanism for how external straining motion in [F1] removes, by ‘vortex stripping’, the low vorticity fluid in the outer boundary part [F2_B] of the vortical region, while the inner core [F2_c] is only slightly distorted. (a) Showing the vortex sheets surrounding [F2] when the straining motion is initiated, and the convergence points X_c where viscous diffusive levels tends to detrainment of vorticity from [F2_B] and (b) shows the displacements of [F2_B] and [F2_c].

large scale vortical motions in the atmosphere and oceans, and in the structure of shear flows with high levels of external turbulence.

We consider the interaction between a compact vortical region and a coplanar straining motion $U(x)$ in the external region [F1], having a length scale L that is large compared with h , and characteristic strain rate U_0/L . See Fig. 8. We make the following assumptions for simplicity; in the core part of [F2], whose length scale is h_c ($\ll h$) and is denoted by [F2_c], the initial vorticity is assumed to be much greater than the external strain rate, so that $\omega_c \gg U_0/L$, and in the much larger outer boundary part of the region, [F2_B], the initial vorticity is much smaller and of order ω_B where $\omega_B < U_0/L$. Note that the velocity here induced by the vorticity in [F2_c] is of order $\omega_c h^2/h_c$. Since $h_c \ll h$, this velocity is smaller than the external velocity $\sim U_0(h/L)$. The interfaces between the core and outer parts of [F2], and between the outer part of [F2] and [F1] are denoted by [B_c] and [B].

The evolution of this flow can be analysed by inviscid vortex dynamics following GI Taylor (see Batchelor, 1967, p. 524) and the theoretical and experimental methods of Rottman et al. (1987).

Imagine that the boundary [B] is rigid up to the time $t=0$ (which leads to a distortion to $\mathbf{U}(\mathbf{x})$) and then dissolved (or consider the flow to be generated by a rapidly growing instability); then a vortex sheet is generated around [B], where $\mathbf{x} = \mathbf{x}^{[S]}$, whose strength $\gamma^*(\mathbf{x}^{[S]})$ varies corresponding to the differences between the initial smaller velocity $u^{[2]}$ on the inside and the larger velocity $\mathbf{U}(\mathbf{x}^{[S]})$ on the outside. This vorticity distribution induces the fluid in the interface to move at approximately $\frac{1}{2}\mathbf{U}(\mathbf{x}^{[S]}, t)$. It affects the velocity field $U(x, t)$ everywhere outside the interface, which now undergoes a large distortion as it follows the direction of the streamlines of the flow in [F1], but does not travel at the same speed. (This is analogous to how, when a cylinder of fluid is suddenly introduced into a cross flow, it distorts itself into a vortex pair and moves downstream at about half the speed of the flow.)

The form of [B] as it moves depends on the relative strengths in the outer part of [F2] of the strain rates induced by the external flow and the core vorticity, indicated by the parameter

$$\Sigma_0 = (U_0/L)(\omega_C h/h_C)$$

If $\Sigma_0 > 1$ much of the fluid and the vorticity in [F2₀] is swept away in two vortices, leaving a trail behind them back to the core vortex. But if $\Sigma_0 < 1$, the fluid and outer vorticity is carried round the core vortex in the form of an elliptical ring. In the latter case, where the core vortex is stronger, the ring can provide some partial sheltering, as explained in Section 3.2.

Note that, although the core vortex is strong enough that its radius is only slightly deformed, by $\sim h\Sigma_0$, it is rotated by a finite angle until it reaches a position of equilibrium where it induces a velocity field that is opposite to that of the strain field. This simple example demonstrates how weaker vorticity can be ‘stripped’ from the outer region of a vortical region by an external straining flow, Legras and Dritschel (1993) have quantified this process for different types of rotational and irrotational straining motion, and shapes, and orientations of the vortical regions. They find results that are consistent with observations of the changing shape of the polar vortex and its accompanying ‘ozone hole’.

The effect of finite amplitude external perturbations ‘stripping’ away the weak vorticity at the outer edge of shear layers has been demonstrated in two earlier laboratory studies. Hancock and Bradshaw (1989) measured the interactions between large-scale free stream turbulence with rms velocity u_0 and length scale L_x and the, outer part (or ‘wake’) of a turbulent boundary layer, whose depth is h . Where the vorticity is ω_B their results show that when $u_0/L_x > \omega_B \sim u^*/h$ (or $u_0 > u^*$ where u^* is the friction velocity or rms turbulence in the boundary layer) the mean vorticity ω_B in the outer part is stripped away and the thickness, and structure, of the boundary layer is reduced to that of the higher shear logarithmic region. Thomas and Simpson (1985) obtained similar results when they measured how the outer shear region of a gravity-current was stripped away by external turbulence when $u_0/L > \omega_B$. The model problem also shows how when vorticity is ‘shed’ from the boundary of a vortical region, it tends to develop into coherent patches of vorticity, as occurs with jets in cross flows (where the flows in the two regions are not coplanar (Coelho and Hunt, 1989)). These may have significant dynamical effects back on the region [F2] it ‘left behind’ and may transport matter and heat away from [F2].

In real, rather than model, complex flows the vortical regions have finite gradients of vorticity, evolve on finite time scales, and at their interface with the external flow viscous diffusion of vorticity

is part of the process of detrainment, or shedding of vorticity. We have considered the first two of these idealisations; what about the third?

Vorticity tends to diffuse from a fluid interface around ‘convergence’ points, denoted by X_c in Fig. 8(b), where the flow parallel to the surface converges, i.e. (in two dimensions) $du^{*[S]}/ds < 0$, and streamlines move into the exterior region [F1] from near the surface. Once a vortical region [F2] has developed into a steady form, if it is located in a unidirectional external flow U , the vorticity that diffuses from near X_c can be advected away from [B]. Because of the converging flow, this detrained vorticity tends to be confined to ‘wakes’ whose width is small compared with h , as is observed below rising vortex rings (Turner, 1973). Therefore in such a flow over most of the exterior side of the interface [B] there is little shed vorticity, so that the large scale interactions and the dynamics determining the response of [F2] to external perturbations is essentially inviscid, as we have assumed. In support of this hypothesis, one notes that in the above example of a deformed vortical region, the detrainment of vorticity by unsteady vortex induced motions is very similar to that produced in a slowly changing flow with viscous diffusion, as is also found in many other flows (e.g. Batchelor, 1967).

The accuracy of the inviscid approximation to these problems in vortex dynamics is even greater if the layer is stretching and rolling up as a result of its own instability and any external perturbations. Since, as explained in Section 2.3 and Batchelor (1967), the rolling up occurs at points X_c where the sheet strength is increased, these potential points of maximum detrainment are also regions where the revolving flow tends to re-entrain any vorticity that escapes (see Hussain and Clark, 1981).

4. Concluding remarks

One of the main uses of research in fluid mechanics is to develop general concepts of value to those working on practical problems and those applying this research in other scientific disciplines. Sometimes these applicable concepts may be little more than labels for a similar group of phenomena, but they are most useful when they include an explanation or mechanism, preferably in familiar terms – the Poincare criterion for a good theory. In this review we have noted that the new questions being asked about many flows of fundamental and practical interest are about the interactions between quite different types of vortical flow structure in adjacent regions, and their sensitivity to variations in initial and boundary conditions. We have shown how in some conditions the two interacting velocity fields can mutually exclude each other across the interface; then, as the conditions vary, the interactions may change markedly so that one of the velocity fields becomes dominant alternatively the two fields may resonate with each other and perhaps cause extra turbulence at the interface.

The understanding and modelling of complex flows is often helped by relating them to idealised flow situations, such as those considered here, and then analysing them with the familiar concepts of vorticity dynamics, especially those of vortex sheets. In high Reynolds number flows the role of viscosity is essential for enabling vorticity to diffuse across the interface between regions because this can change the large scale velocity field; however the global effects of this vorticity diffusion can be significant even though the diffusion process is quite localised near convergence points on the interfaces.

Metaphorical terms are useful for describing and classifying some of the striking effects in these situations, such as blocking, shear sheltering and vortex stripping. They may be useful for suggesting

hypotheses to motivate new studies, or as a useful checklist of phenomena which any given model should describe. It is notable that several models for engineering and environmental flows which currently do not describe these phenomena well.

Acknowledgements

JCRH is grateful to the Japanese Society for Fluid Mechanics for inviting him to attend their 30th anniversary meeting, and, for supporting the research reported here, to Arizona State University Fluid Mechanics Program (with funding from the US National Science Foundation) and the Center for Turbulence Research at Stanford University and NASA Ames. We have learnt much from many conversations with colleagues, especially N.K.R. Kevlahan, J.C. Vassilicos, I. Eames, R. Jacobs, X. Wu, A.F.M. Hussain, H.J.S Fernando, T. Miyazaki. We acknowledge useful comments by the referees.

References

- Batchelor, G.K., 1967. *Introduction to Fluid Dynamics*. Cambridge University Press, Cambridge.
- Bisset, D.K., Cai, X., Hunt, J.C.R., Rogers, M., 1998. The local structure of the turbulent/non-turbulent interface of shear flows. Annual report from CTR Stanford University.
- Britter, R.E., Hunt, J.C.R., Mumford, 1979. The distortion of turbulence by a circular cylinder. *J. Fluid Mech.* 92, 269–301.
- Carruthers, D.J., Hunt, J.C.R., 1986. Velocity fluctuations near an interface between a turbulent region and a stably stratified layer. *J. Fluid Mech.* 165, 475–501.
- Ching, C.Y., Fernando, H.J.S., Robles, A., 1995. Breakdown of line plumes in turbulent environments. *J. Geophys. Res. (Oceans)* 100 (C3), 4707–4713.
- Coelho, S.L.V., Hunt, J.C.R., 1989. Vorticity dynamics in the near field of strong jets in crossflows. *J. Fluid Mech.* 200, 95–120.
- Collier, C.G., Dixon, J., Harrison, M.S.J., Hunt, J.C.R., Mitchell, J.F.B., Richardson, D.S., 1994. Extreme surface winds in mid-latitude storms: Forecasting changes in climatology. *J. Wind Eng. Ind. Aerodyn.* 52, 1–27.
- Craik, A.D.D., 1991. The continuous spectrum of the Orr–Sommerfeld equation: note on a paper of Grosch and Salwen. *J. Fluid Mech.* 226, 565–571.
- Davidson, M.J., Mylne, K.R., Jones, C.D., Phillips, J.C., Perkins, R.J., Fung, J.C.H., Hunt, J.C.R., 1995. Plume dispersion through large groups of obstacles – a field investigation. *Atmos. Environm.* 29, 3245–3256.
- Drazin, P.G., Reid, W.H., 1980. *Hydrodynamic Stability*. Cambridge University Press, Cambridge.
- Fernando, H.J.S., Hunt, J.C.R., 1997. Turbulence, waves and mixing at shear-free density interfaces. Part 1. A theoretical model. *J. Fluid Mech.* 347, 197–234.
- Ferré, J.A., Mumford, J.C., Savill, A.M., Giralt, F., 1990. Three-dimensional large-eddy motions and fine-scale activity in a plane turbulent wake. *J. Fluid Mech.* 210, 371–414.
- Ffowcs-Williams, J.E., Purshouse, M., 1981. A vortex sheet modelling of boundary layer noise. *J. Fluid Mech.* 113, 187–220.
- Gartshore, I.S., Durbin, P.A., Hunt, J.C.R., 1983. The production of turbulent stress in a shear flow by irrotational fluctuations. *J. Fluid Mech.* 137, 307–329.
- Goldstein, M.E., Wundrow, D.W., 1998. On the environmental realisability of algebraical disturbances and their relation to Klebanoff modes. *Theoret. Comput. Fluid Dyn.* 10, 171–186.
- Grosch, C.E., Salwen, H., 1978. The continuous spectrum of the Orr–Sommerfeld equation, Part I – The Spectrum and the eigen function. *J. Fluid Mech.* 68, 33.
- Hancock, P.E., Bradshaw, P., 1989. Turbulence structure of a boundary layer beneath a turbulent free stream. *J. Fluid Mech.* 205, 45–76.

- Hodson, H.P., 1985. Measurements of wake-generated unsteadiness in the rotor passages of axial flow turbines. *J. Eng. Gas Turb. Power* 107, 467.
- Hunt, J.C.R., 1998. Qualitative questions in fluid mechanics. *Appl. Sci. Res.* 58, 483–501.
- Hunt, J.C.R., Carruthers, D.J., 1990. Rapid distortion theory and the ‘problems’ of turbulence. *J. Fluid Mech.* 212, 497–532.
- Hunt, J.C.R., Graham, J.M.R., 1978. Free-stream turbulence near plane boundaries. *J. Fluid Mech.* 84, 209–235.
- Hunt, J.C.R., Perkins, R.J., Fung, J.C.H., 1995. Problems in modelling disperse two-phase flows. Presented to the 12th U.S. National Congress of Applied Mechanics. *Appl. Mech. Rev.* 47 (6) Part 2, S49–S60.
- Hunt, J.C.R., Vassilicos, J.C., 1993. Kolmogorov’s contributions to the physical and geometrical understanding of small scale turbulence and recent developments. *Proc. Roy. Soc. Special ed.* 1991, 434, 183–210.
- Hussain, A.K.M.F., Clark, A.R., 1981. On the coherent structure of the axisymmetric mixing layer: a flow-visualization study. *J. Fluid Mech.* 104, 263–294.
- Jackson, P.S., 1981. On the displacement height in the logarithmic velocity profile. *J. Fluid Mech.* 111, 15–25.
- Jacobs, R.G., Durbin, P.A., 1998. Shear sheltering and the continuous spectrum of the Orr–Sommerfeld equation. *Phys. Fluids* 10, 2006–2011.
- Kevlahan, N.K.R., Farge, M., 1997. Vorticity filaments in two-dimensional turbulence; creation, stability and effect. *J. Fluid Mech.* 346, 49–76.
- Kevlahan, N.K.R., Hunt, J.C.R., 1997. Non-linear interactions in turbulence with strong irrotational. *J. Fluid Mech.* 337, 333–364.
- Koch, D., 1993. Hydrodynamic diffusion in dilute sedimenting suspensions at moderate Reynolds numbers. *Phys. Fluids A* 5, 1141, 1993.
- Legras, B., Dritschel, D., 1993. Vortex stripping and the generation of high vorticity gradients in two-dimensional flows. *Appl. Sci. Rep.* 51, 445–455.
- Lighthill, M.J., 1957. The fundamental solution for small steady three-dimensional disturbances to a two-dimensional parallel shear flow. *J. Fluid Mech.* 2, 493–512.
- Liu, X., Rodi, W., 1991. Experiments on transitional boundary layers with wake-induced unsteadiness. *J. Fluid Mech.* 231, 229–256.
- Lundgren, T.S., 1982. Strained spiral vortex model for turbulent fine structure. *Phys. Fluids* 25, 2193–2203.
- Magnaudet, J., Rivero, M., Fabre, J., 1995. Accelerated flows past a rigid sphere or a spherical bubble, Part I. Steady streaming flow. *J. Fluid Mech.* 284, 97–135.
- Marshall, J.S., 1997. The flow induced by periodic vortexing wrapped around a columnar vortex core. *J. Fluid Mech.* 345, 1–7.
- Methven, J., Hoskins, B.J., 1998. Spirals in potential vorticity, Part I. Measures of structure. *J. Atmos. Sci.* 55, 2053–2066.
- Miyazaki, T., Hunt, J.C.R., 1998. Turbulence structure around a columnar vortex; rapid distortion theory and vortex wave excitation. In: Frisch, U. (Ed.), *Proc. European Turbulence Conf. (ETC-7)*, Kluwer, Dordrecht, pp. 373–376.
- Moffat, H.K., Kida, S., Okhitani, K., 1995. Stretched vortices – the sinews of turbulence; large-Reynolds-number asymptotics. *J. Fluid Mech.* 259, 241–264 (and Corrigendum, 266, 371).
- Nakamura, L., Kershaw, R., Grait, N., 1996. Prediction of near-surface gusts generated by deep convection. *Meteor. Appl.* 3, 157–167.
- Perera, M.J.A.M., Fernando, H.J.S., Boyer, J.L., 1994. Turbulent mixing at a inversion layer. *J. Fluid Mech.* 267, 275–298.
- Perot, B., Moin, P., 1995. Shear free turbulent boundary layers. Part I. Physical insights into near wall turbulence. *J. Fluid Mech.* 295, 199–245.
- Phillips, O.M., 1955. The irrotational motion outside a free boundary layer. *Proc. Cambridge. Phil. Soc.* 51, 220.
- Rotach, M.W., 1993. Turbulence close to a rough urban surface. *Boundary-Layer Meteorol.* 65, 1–28.
- Rottman, J.W., Simpson, J.E., Stansby, P.K., 1987. The motion of a cylinder of fluid released from rest in a cross flow. *J. Fluid Mech.* 177, 307–337.
- Saffman, P.G., 1992. *Vortex Dynamics*. Cambridge University Press, Cambridge.
- Tatsumi, T., 1999. Fluid Mechanics in the turn of the century. These proceedings, *Fluid Dyn. Res.* 24, 315–319.
- Terry, P.W., Newman, D.F., Matter, N., 1992. Coherence of intense localised vorticity in decaying two-dimensional Navier–Stokes turbulence. *Phys. Fluids A* 5, 927–937.
- Thomas, N.H., Simpson, J.E., 1985. Mixing of gravity currents in turbulent surroundings. In: Hunt, J.C.R. (Ed.), *Turbulence and Dispersion in Stable Environments*. Clarendon Press, Oxford, pp. 61–95.
- Townsend, A.A., 1976. *The structure of turbulent shear flow*. Cambridge University Press, Cambridge.

- Turner, J.S., 1973. *Bouyancy Effects on Fluids*. Cambridge University Press, Cambridge.
- Veeravalli, Warhaft, Z., 1989. The shearless turbulent mixing layer. *J. Fluid Mech.* 207, 191–229.
- Versicco, R., Jimenez, J., Orlandi, P., 1995. On steady columnar vortices under local compression. *J. Fluid Mech.* 289, 367–387.
- Voke, P.R., Yang, Z., 1995. Numerical study of bypass transition. *Phys. Fluids* 7, 2256–2264.
- Wu, X., Jacob, R., Hunt, J.C.R., Durbin, P., 1999. Simulation of a boundary layer transitions induced by periodically passing wake. *J. Fluid Mech.* (in press).